J. Physiol. (Paris) 94 (2000) 445–463

PII: S0928-4257(00)01084-6/FLA

Dynamics of networks of randomly connected excitatory and inhibitory spiking neurons

Nicolas Brunel*

LPS (Laboratory associated with CNRS, Paris 6 and Paris 7 Universities), École normale superieure, 24, rue Lhomond, 75231 Paris Cedex 05, France

Abstract – Recent advances in the understanding of the dynamics of populations of spiking neurones are reviewed. These studies shed light on how a population of neurones can follow arbitrary variations in input stimuli, how the dynamics of the population depends on the type of noise, and how recurrent connections influence the dynamics. The importance of inhibitory feedback for the generation of irregularity in single cell behaviour is emphasized. Examples of computation that recurrent networks with excitatory and inhibitory cells can perform are then discussed. Maintenance of a network state as an attractor of the system is discussed as a model for working memory function, in both object and spatial modalities. These models can be used to interpret and make predictions about electrophysiological data in the awake monkey. © 2000 Elsevier Science Ltd. Published by Éditions scientifiques et médicales Elsevier SAS

network / models / noise / dynamics / synchronization / inhibition / irregularity / integrate-and-fire neurone / attractor dynamics / working memory

1. Introduction

The dynamics of networks of spiking neurones have received in the last decade a large amount of interest from theorists. Early studies focused on fully connected and noiseless systems [1, 28, 33, 34, 39, 48, 65, 69], or locally coupled systems [43, 64]. In these systems, the dynamics generally converges to states in which neurones behave like oscillators. The main question is to determine whether the network settles in a synchronous or asynchronous state. More recently, several groups have investigated network states in which neurones fire irregularly — a situation much closer to neuronal networks in vivo [5, 67, 70, 71]. Irregular firing tends to occur in networks with some kind of strong synaptic disorder, as in sparsely connected networks, generally in presence of strong inhibition. van Vreeswijk and Sompolinsky [70] studied the properties of 'chaotic balanced states' in a network of binary neurones. More recently, analytical studies have revealed the properties of the simplest spiking neuronal network models, i.e. networks of integrate-and-fire neurones [12, 15]. These networks have a very rich dynamics, even when no spatial structure and no synaptic dynamics are present. In particular, oscillatory states in which neurones fire irregularly at rates lower than the network frequency often occur. These oscillations resemble oscillatory phenoma observed in the hippocampus both in vivo [19, 25] and in vitro [18, 29].

Once the dynamics in systems with no connection structure is well understood, it is interesting to study the dynamics of networks with structure in the recurrent connections. Structured recurrent connections are known to endow neural networks with interesting computational properties. In particular, the computational role of recurrent connections has been extensively studied in recent years in the context of the visual system [9, 61, 67]. Recurrent connections are also useful to model working memory properties. Models of working memory are interesting because they can potentially bridge the gap between cellular neurophysiology and electrophysiological experiments in monkeys performing working memory tasks. In these tasks, persistent (significantly higher than spontaneous) activity is observed in cells in various areas in association cortices during the delay period during which monkeys have to maintain an item or a spatial location in working memory. This phenomenon (also called delay activity or mnemonic activity) is widely believed to subserve the cellular correlate of working memory. In the ventral stream, neurones exhibit delay activity for objects such as faces, fruits, or fractal patterns, in IT cortex [32, 47, 49, 59], perirhinal and entorhinal cortices [63], and in the ventral part of the prefrontal cortex [51, 52]. In the dorsal stream, neurones whose persistent activity is related to a memorized

* Correspondence and reprints.
E-mail address: brunel@lps.ens.fr (N. Brunel).

spatial location have been observed in parietal cortex as well as prefrontal cortex [21, 30]. Recently, implementations of old ideas about associative memory models in networks of excitatory and inhibitory spiking neurones have been proposed [5, 24]. These models, when endowed with specific synaptic structures, can function as working memory networks and show remarkable similarities with experimental data [3, 24, 76].

The first part of this paper will be concerned with results concerning the dynamics of neurones with either no recurrent connections, or random and structureless recurrent connections. Then, in the second part, examples in which structure in the recurrent connections endows the network with working memory properties will be discussed.

2. Materials and methods

2.1. The cortical circuit model

The cortical circuit model is composed of a large number of pyramidal cells (80%) and interneurones (20%). Each cell receives a large number of recurrent connections, but connections are not all-to-all. Rather, considered networks have a connection probability of order ~ 1–10%. All types of connections exist (i.e. pyramidal to pyramidal, pyramidal to interneurone, interneurone to pyramidal, interneurone to interneurone). Each cell receives a large number of long range connections from outside the circuit, which are assumed to be purely excitatory.

Due to the low connection probability, the network will sometimes be called 'sparsely connected'. The orders of magnitude we consider are networks of hundreds of thousands of neurones, each neurone being connected to about ten thousand cells. Thus, results should apply to areas such that the CA3 network of the hippocampus and local neocortical networks (see e.g. [62]). *Figure 1* gives a simplified sketch of such a network.

2.2. Neurones and synapses

Both pyramidal cells and interneurones are modelled as integrate-and-fire neurones. Neurone i is described by its membrane potential $V_i(t)$. The membrane potential obeys, below threshold ($V_i(t) < \theta$), to

$$\tau g_{\text{leak}} V_i = g_{\text{leak}}(V_{\text{rest}} - V_i) + I_i \qquad (1)$$

where τ is the integration time constant, V_{rest} the resting potential, g_{leak} the leak conductance of the cell, and I_i the total synaptic current. The simplest model for synaptic currents one can think of is

$$I_i(t) = \text{synaptic input} = \tau \sum_j J_j \sum_k \delta(t - \delta - t_j^k)$$

where the sum over j corresponds to a sum on all synapses of the neurone, J_j represents the amplitude of the postsynaptic potential elicited by synapse number j, the sum over k corresponds to a sum over spikes arriving at a given synapse, and the individual postsynaptic response is described by a delta function occurring at a time δ (a transmission delay) after the presynaptic spike. Such synapses will be called 'delta' synapses in the following. A more realistic description of synaptic currents would be to incorporate a synaptic current decay time constant τ_{syn}. In that case, the synaptic current is no longer instantaneous, but rather jumps to a finite value at a time δ after the presynaptic spike, and then decays exponentially with a time constant τ_{syn}. Such a synapse will be called 'exponential' in the following. Both types of synaptic currents provoked by a single spike are shown in *figure 2*.

Spike emission occurs when $V_i(t) \geq \theta$. The potential then comes back to V_r after an ARP τ_0. Cortical neurones in vivo receive a huge bombard-

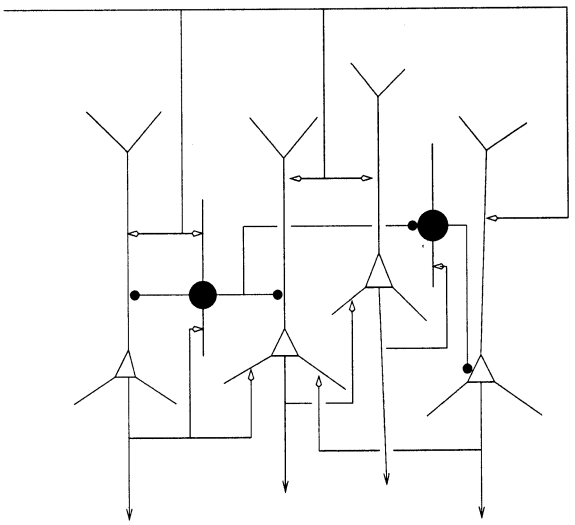

Figure 1. A simplified recurrent circuit model. Pyramidal cells (open triangles) and interneurones (black circles) are connected through synapses (glutamatergic synapses in open arrows, GABAergic synapses in black circles). Both types of cells receive glutamatergic long range connections. Adapted from [62].

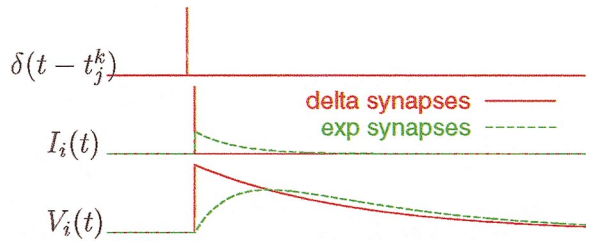

Figure 2. Synaptic currents and postsynaptic potentials due to the arrival of a single spike. In red, 'delta' synapses are described by delta function synaptic currents, and a instantaneous jump of the membrane potential followed by exponential decay. In green, 'exponential' synapses make an instantaneous jump to the peak current, followed by an exponential decay. Postsynaptic potential is described by a difference of exponentials.

ment of excitatory and inhibitory presynaptic spikes due to spontaneous and/or stimulus related activity, through synapses which are weak compared to the distance between resting potential and the firing threshold. In such a situation (*figure 3*), the membrane potential of the neurone does something that looks like a random walk, until it hits threshold. Consequences of synaptic bombardment on neuronal properties have been studied by a number of authors [10, 27, 55].

2.3. Towards more realistic synaptic models

In recurrent networks, synaptic interactions determine to a large extent the collective properties of the network. It is therefore of crucial importance to understand how details of the implementations of synaptic models affect the network behaviour. Synaptic models, as network models, have various levels of complexity (for a review see [26]). A possible realistic implementation of synaptic currents was proposed by Wang [72], based on slice data. In that implementation, three types of synaptic currents are present: GABA, AMPA, and NMDA-receptor mediated currents.

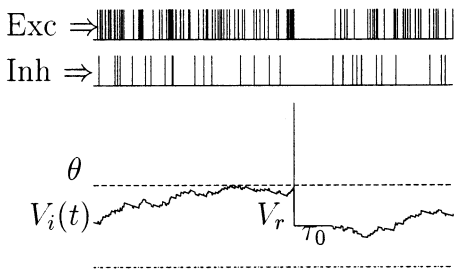

Figure 3. Response of an integrate-and-fire neurone to Poisson trains of excitatory and inhibitory spikes.

All synaptic currents are of the form $I_{syn}(t) = g_{syn}(V_{rev}-V(t))s(t)$, where V_{rev} is the reversal potential, g_{syn} is the maximal conductance (possibly voltage-dependent), and s is the fraction of open channels at time t, describing the time course of the post-synaptic current (PSC).

Three types of PSC time courses are commonly used in the literature (see e.g. [33]). 'Delta' (or 1-step) synapses have a single time constant associated with it: a latency δ. 'Exponential' (or 2-step) synapses are described by a latency δ, and a decay time τ_{decay}. 'Difference of exponential' (or 3-step) synapses are described by a latency, a rise time τ_{rise} and a decay time τ_{decay}.

Specifically, in the implementation of Wang [72], $GABA_A$ is described by $I_{syn}(t) = g_{GABA}(V-V_I)s(t)$ where $s(t)$ has decay time 10 ms. AMPA is described by $I_{syn}(t) = g_{AMPA}(V-V_E)s(t)$ with a decay time 2 ms, and NMDA by $I_{syn}(t) = g_{NMDA}(V-V_E)s(t)$, where $s(t)$ has a rise time 2 ms and decay time 100 ms, saturates at rather low presynaptic frequencies, and the conductance gNMDA has a nonlinear voltage dependence due to $[Mg^{2+}]$ block [44].

2.4. Summary of parameters

2.4.1. 'Simple' model

In the simple model, inhibitory and excitatory neurones have the same intrinsic parameters (i.e. integration membrane time constant, amplitude of EPSPs and IPSPs). The parameters defining the network are:

- Number of pyramidal cells $N_E = 0.8N$, of interneurones $N_I = 0.2N$, where N is assumed very large;
- Integration time constant $\tau = 20$ ms;
- Other neuronal parameters are $\theta = 20$ mV; $V_r = 10$ mV; $\tau_{rp} = 2$ ms;
- The EPSP amplitude is in the range $J \approx 1$–1 mV $\rightarrow \theta/J \ll 1$;
- Number of recurrent excitatory connections $C_E \sim 1\,000$–$10\,000$, $C_I \sim C_E/4$;
- Synaptic delay $\delta \sim 1$–2 ms;
- Strength of inhibitory synapses g relative to the strength of excitatory synapses;
- Total background frequency of external inputs to a cell $C_{ext}\nu_{ext}$ relative to the frequency needed to bring cells to firing threshold $C_{ext}\nu_{thr}$.

These two last parameters will be varied systematically in the following. They are in practice the most important parameters controlling the dynamics. In the first part of the present paper (up to section 3.3) unstructured networks in which pyra-

midal cells and interneurones have identical characteristics are considered. A detailed study of the dynamics in the more realistic case in which these two types of cells have different characteristics is done in [12].

2.4.2. 'Realistic' model

In the 'realistic' model, interneurones have a smaller integration time constant than pyramidal cells (10 vs. 20 ms), a smaller refractory time period (1 vs. 2 ms). Synaptic interactions are as specified in Section 2.3.

2.5. Analytical methods

The simplicity of IF neurones makes it possible to study the system analytically. Thus, the properties of the network can be determined mathematically, rather than simulated numerically. In the following, the main ideas underlying the calculations are outlined. The interested reader can find details in [5, 12, 15].

2.5.1. Diffusion approximation

The first step is to look at *figure 2* (or at intracellular recordings in vivo) and realize that the dynamics of the membrane potential looks very much like a random walk. This the case because EPSP and IPSP amplitudes are small compared to threshold (rough estimates in cortex would be $J/\theta \sim 0.005$–0.05), and because of the high frequency of spikes impinging to the neurone due to the large number of connections. The idea behind the diffusion approximation is to replace a complicated process, the synaptic input, which is a sum over discrete events, by a continuous process that is much simpler to manage, and 'looks' very similar to the original one. In mathematical terms, it will be required that the two first moments (mean and correlation function) of the two processes be equal. In the case of δ synapses, the synaptic input can be approximated in that way by the sum of a population-averaged current plus a white noise describing the fluctuations in the synaptic inputs from neurone to neurone. In the case of exponential synapses the synaptic input can be replaced by an average current plus a coloured noise, which, unlike the white noise, has a correlation time which is equal to the synaptic time.

2.5.2. Description of the population dynamics (white noise case)

In the diffusion approximation, the equation describing the evolution of the membrane potential (1) becomes a Langevin equation [8, 68]. It is known that this equation can be converted to the so-called Fokker-Planck equation that describes the time evolution of the spatial distribution of membrane time potentials (see e.g. [58]). In that formalism, the probability to find the potential V at time t is defined as $P(V,t)$. The probability of firing at time t is defined as $\nu(t)$. These probabilities apply either to a single cell, or to a population of identical cells receiving the same deterministic component, provided the external noise is uncorrelated from cell to cell.

$P(V,t)$ obeys a Fokker-Planck equation

$$\tau P(V,t)t = \frac{\sigma^2(t)}{2}\frac{\partial^2 P(V,t)}{\partial V^2} + \frac{\partial}{\partial V}[(V-\mu(t))P(V,t)] \quad (2)$$

where $\mu(t)$ is the mean synaptic input at time t, while $\sigma^2(t)$ is the variance of noise at time t. In the case of networks without recurrent connections, these parameters correspond to external contributions (i.e. external stimuli) only. When recurrent connections are added, these parameters will become a sum of two contributions, one from outside, one from the network itself through recurrent collaterals.

The boundary conditions of the partial differential Eq. (2) give the firing probability of the population. At the firing threshold θ, an absorbing boundary condition is needed, and the firing probability $\nu(t)$ is given by the probability flux at θ

$$P(\theta,t) = 0, \frac{\partial P}{\partial V}(\theta,t) = -\frac{2\nu(t)\tau}{\sigma^2(t)}$$

At the reset potential V_r, the condition is that what comes out at θ must come in at V_r

$$P(V_r^-,t) = P(V_r^+,t), \frac{\partial P}{\partial V}(V_r^-,t) - \frac{\partial P}{\partial V}(V_r^+,t) = -\frac{2\nu(t)\tau}{\sigma^2(t)}$$

The dynamics of the system has now been fully specified. The next step is to solve these equations. In the Section 3, solutions to these equations are described in three cases.

2.5.3. No recurrence, stationary inputs

When the input is stationary, $\mu(t) = \mu_0$, $\sigma(t) = \sigma_0$. One has then to look for time-independent solutions of Eq. (2).

2.5.4. No recurrence, time-varying inputs

Suppose now that an arbitrary time-varying stimulus $\mu(t)$ is received by the neurone. What is

the dynamics of the population firing rate $\nu(t)$ in response to that stimulus? To tackle this problem, it is useful to start with a small periodic modulation of a constant stimulus with frequency ω, $\mu(t) = \mu_0 + \mu_1 \exp(i\omega t)$, $\mu_1 \ll \mu_0$.

In response to such a stimulation, the neurone will emit spikes with firing probability $\nu(t)$

$$\nu(t) = \nu_0 + \nu_1(\omega)\mu_1 \exp(i\omega t), \quad \nu_1 \ll \nu_0$$

$\nu_1(\omega)$ is the linear response of the population at frequency ω (*figure 4*).

The usefulness of this function of the frequency is that one can then reconstruct the response of the system to an arbitrary stimulus with small temporal variations:

$$\mu(t) = \mu_0 + \int d\omega \mu_1(\omega) \exp(i\omega t) \rightarrow$$

$$\nu(t) = \nu_0 + \int d\omega \nu_1(\omega)\mu_1(\omega) \exp(i\omega t)$$

Thus, this is the basic quantity which will be used to probe the dynamics of a system of neurones. In particular, the behaviour at high frequency is interesting because it tells us how fast the system will react to fast changes in the inputs.

The same formalism can be applied when the noise amplitude σ, rather than the deterministic part σ, is modulated periodically, yielding a different linear response function $\nu_\sigma(\omega)$ (see also [11]).

2.5.5. Intrinsic dynamics of the randomly connected recurrent network

Until this point, networks without recurrent connections have been considered. Introducing recurrent connections introduces interesting dynamical phenomena. For example, some temporal structure might appear in the population firing rate even when the external inputs are constant. Recurrent connections of course complicate the analysis. Essentially three limit cases have been studied in the literature. The first consists in the homogeneous, all-to-all coupled network (see e.g. [1, 23, 33, 34, 39, 48, 66]). The second concerns locally coupled networks (e.g. [43]). Last, sparsely connected networks, defined here as networks with a small connection probability between neurones, have been studied more recently [12, 15, 36, 53, 70, 71].

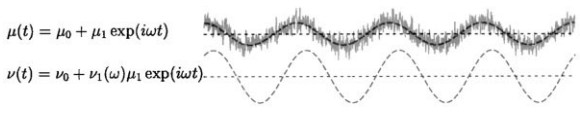

Figure 4. A noisy synaptic input with a small sinusoidal component (upper trace) generates a population firing rate with a small sinusoidal component (lower trace).

In the following, the focus will be on the sparsely connected network. There are two main reasons to consider these networks rather than other kind of architectures: (1) they are closer to real local cortical networks than all-to-all or locally coupled networks; (2) the fact that the connection probability between cells is small makes feasible an analytical study.

For networks with a large number of connections but a small connection probability, a systematic study of the dynamics was first performed with binary neurones by van Vreeswijk and Sompolinsky [71]. Then, the dynamics of such networks with integrate-and-fire neurones and delta synapses have been studied by Brunel and Hakim [12, 15]. Briefly, the analytical strategy consists in the following steps

1. Determine the stationary (asynchronous) states of the system, by setting $\partial P/\partial t = 0$ in Eq. (2) and finding an explicit solution [5, 15]. These states are characterized by a stationary firing probability of the populations composing the network. The network state is asynchronous. However, these states are not necessary stable.
2. Perform a linear stability analysis of the stationary states [12, 15]. In this way, one usually determines oscillatory instability (Hopf bifurcation) lines in parameter space. Crossing these instability lines means that a global oscillation develops in which the firing probability of the neuronal populations is no longer constant but rather oscillates in time. The states can be called synchronized oscillatory states.
3. In addition, weakly non-linear analysis. Such an analysis can tell us in more detail what is the network behaviour in synchronous states close to the bifurcation, as for example the nature of the bifurcation (sub or super critical), and how the amplitude and the frequency of the oscillation vary moving away from the bifurcation [15].
4. The last step is to study finite connection probability effects. In a finite network, the transition between synchrony and asynchrony is smooth, as is typically the case in stochastic dynamics. Thus, damped oscillatory behaviour appear in stationary states close to the bifurcation lines, and phase diffusion effects appear in oscillatory states. These effects can be quantitatively determined [15].

2.6. Computation in recurrent circuits: models of working memory

Recurrent circuits can potentially perform many interesting computations. In a particular class of models, the network has a repertoire of attractors, which may have a point-like structure, or have the topology of a circle, a line, or higher dimensional structures. The external inputs typically select one out of many possible attractors. The selection of one attractor out of many can be seen as 'recognition' of an external input which may be seen as being 'stored' in the synaptic structure. The persistence of the network state in an attractor between stimulus presentations can be seen as a mechanism for 'working memory'.

In the following, several models based on the cortical architecture described in Section 2.1 that have been studied as models for working memory function are briefly described. Interestingly, these models can be compared in some detail with data obtained in neurophysiological experiments in the awake monkey (see e.g. [3, 24, 76]). For other recent investigations of attractor network dynamics, see [38, 60].

2.6.1. Architecture of an object working memory model

Models for associative memory using the idea of attractor dynamics have been present in the literature for a long time (see e.g. [2, 41, 74]). In these models, objects are stored in the synaptic matrix using 'learning rules' which are all related to some extent to Hebb ideas [40]. Such models using binary neurones were studied extensively by physicists [7, 2]. In a series of papers, Amit and collaborators [3, 5, 8] studied extensions of these models with more realistic characteristics, and showed that these models could account for many features of neurophysiological data in IT cortex of the behaving monkey during delayed match to sample tasks [49, 50].

The model studied by Amit and Brunel [5] is based on the cortical network architecture introduced in Section 2.1. The additional feature that allows the network to function as a working memory device is to assume a suitable structure in the synaptic connections which is correlated with objects shown to the network. An 'object' is defined at the network level by the response of cells during its presentation. In the simplest model, (shown in *figure 5*), a particular object activates a particular sub-population of the cells of the network. Different objects activate non-overlapping populations of cells.

The model of Amit and Brunel [5] then assumes a very simple synaptic structure: synapses connecting two neurones that are activated by the same object are stronger than average. Cells connecting neurones that are activated by different objects are weaker than average. Such a synaptic structure, illustrated in *figure 5*, can be generated by a simple stochastic learning mechanism using LTP and LTD-like transitions between synaptic states [4, 6, 13].

2.6.2. Architecture of a spatial working memory network

A model for spatial working memory has been proposed in the context of networks of firing rate neurones by [20]. The synaptic structure in such networks is similar to models of orientation columns in visual cortex [9, 61, 67], or models of head direction cells [56].

Compte et al. [24] investigated the implementation of such a synaptic structure on top of the cortical network architecture presented in Section 2.1. It is shown in *figure 6*. Neurones are spatially distributed according to the stimulus to which they are most sensitive (preferred cue in an oculomotor delayed response task [30]) and their collaterals may differentially target neighbouring (isodirectional) and distant (crossdirectional) neurones. Cells receive external synaptic inputs which are selective to the angle of the peripheral cue during its presentation. Each model neurone is labelled by its preferred cue position (an angle), and neurones of the network cover uniformly all the angles along a circle. Therefore, the cells are spatially distributed on a ring and their position in the ring has a linear relationship with their preferred cue angle.

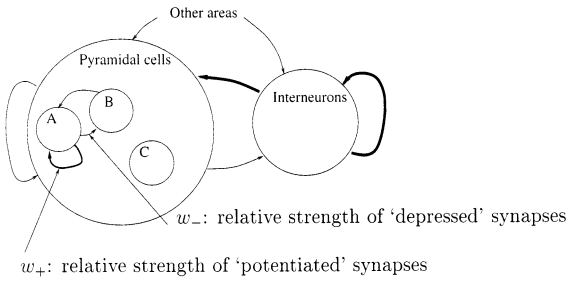

Figure 5. Architecture of a model for object working memory. For more details see text and [5].

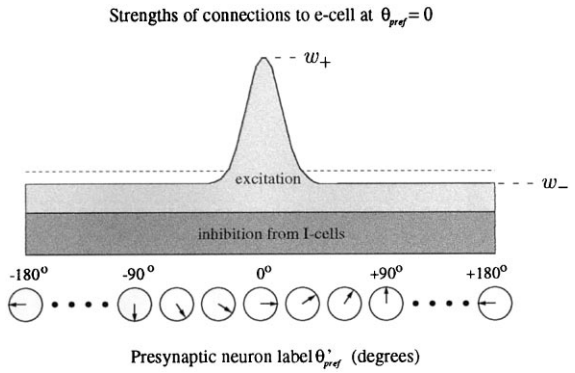

Figure 6. Architecture for a model of spatial working memory. The synaptic connection strength decreases with the difference in the preferred cues of two neurones, with strong interactions between neighbouring neurones and weak interactions between more distant neurones. Adapted from [24]. More details in text and in Compte et al. [24].

3. Results

3.1. No recurrence, stationary stimuli

3.1.1. White noise: f-I curve

The following results can be obtained when the input to a cell is constant, e.g. $\mu(t)=\mu_0$, $\sigma(t)=\sigma_0$:

The stationary probability density of membrane potentials is given by

$$P_0(V)=2\frac{\nu_0 T}{\sigma_0}\times \exp\left(-\frac{(V-\mu_0)^2}{\sigma_0^2}\right)\int_{\frac{V-\mu_0}{\sigma_0}}^{\frac{\theta-\mu_0}{\sigma_0}}\Theta(u-V_r)\exp(u^2)\mathrm{d}u$$

The stationary firing probability is [57]

$$\frac{1}{\nu_0}=\tau\sqrt{\pi}\int_{\frac{V_\tau-\mu_0}{\sigma_0}}^{\frac{\theta-\mu_0}{\sigma_0}}du\exp(u^2)(1+\mathrm{erf}(u))$$

Plotting the curve ν as a function of the mean current μ, for a given noise level σ, corresponds to plotting the f-I curve of a neurone with a given noise level. Such a f-I curve is shown in *figure 7*. Note that in presence of noise such a curve shows two distinct regimes: a sub-threshold regime (shown in lower right panel) in which neurones fire irregularly, and a supra-threshold regime (shown in upper right panel), in which neurones fire more regularly.

It is also possible to compute the coefficient of variation of the inter-spike intervals (ISI) [12, 68]. This coefficient is of order 1 (indicating a Poisson-like process) in the sub-threshold regime. It is typically much smaller than 1 in the supra-threshold regime.

3.1.2. Constant current plus coloured synaptic noise

Noise experienced by neurones in the cortex is not white. Realistic noise models should have a correlation time, since synaptic noise has temporal correlations due to the finite width of postsynaptic currents. Such a noise can be mathematically described by a coloured noise, in which a correlation time τ' appears. Coloured noise complicate significantly calculations. Indeed, it is no longer possible to find an exact solution of the stationary probability density and firing probability. Rather, one

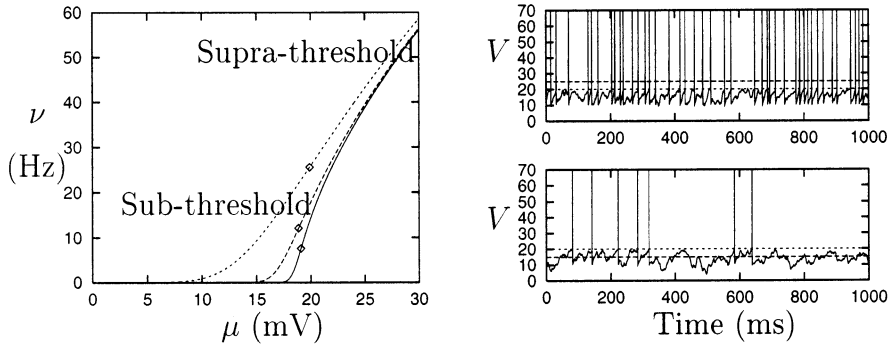

Figure 7. Left: The f-I curve (transfer or response function). Output frequency $\nu=\phi(\mu,\sigma)$ as a function of μ (in mV), for three values of the fluctuation parameter $\sigma=1$ mV (full line), 2 mV (long dashed line), 5 mV (short dashed line). Upper right: Example of a neurone in the supra-threshold firing mode ($\mu>\theta$), in which firing is driven primarily by the mean synaptic inputs. Lower right: Example of a neurone in the sub-threshold firing mode, in which firing is driven by fluctuations around the mean input. In the right panels, spikes are represented as vertical bars between 10 and 70 mV above resting potential.

can perform calculations in some limit cases. An interesting limit which is amenable to analysis, using results of mathematical physics [37, 45], is when the correlation time of the noise τ' is much smaller than the membrane time constant.

In the following, the main ideas behind the calculation and the results are outlined. The reader interested in mathematical details may consult [16]. The population is now described by the probability of finding the potential of a neurone at V and the synaptic current at I at time t $P(V,I,t)$ whose time evolution obeys to

$$\tau' \frac{\partial P}{\partial t} = \frac{\sigma^2(t)}{2} \frac{\partial^2 P}{\partial I^2} + \frac{\partial}{\partial I}[(I-\mu(t))P] + -\frac{\tau'}{\tau} \frac{\partial}{\partial V}[(V-I)P]$$

The boundary conditions are now more complicated. These conditions are actually what makes the problem much more difficult than the problem in the white noise case. The boundary condition at threshold θ is:

- For $I > \theta$, $\tau v(I) = (I-\theta)P(\theta,I)$
- For $I < \theta$, $P(\theta,I) = 0$

At reset potential V_r, the condition is again that what comes out at θ must come in at V_r

- For $I > \theta$, $P(V_r^+,I) = P(V_r^-,I) + P(\theta,I)$
- For $I < \theta$, $P(V_r^+,I) = P(V_r^-,I)$

In the limit $\tau' \ll \tau$, the stationary firing probability is, for $\tau_{rp} = 0$,

$$\frac{1}{\nu_0} = \tau\sqrt{\pi} \int_{\frac{V_r-\mu_0}{\sigma_0}+\alpha\sqrt{\frac{\tau'}{\tau}}}^{\frac{\theta-\mu_0}{\sigma_0}+\alpha\sqrt{\frac{\tau'}{\tau}}} du \exp(u^2)(1+\mathrm{erf}(u)) \qquad (3)$$

where $\alpha = |\zeta(1/2)|/\sqrt{2} \approx 1.03$ and ζ is Riemann's zeta function [16].

Qualitatively, the properties of the f-I curve are unchanged.

3.2. No recurrence, time varying stimuli

3.2.1. No noise

The dynamics of a population of cells in the noiseless case was first studied by Knight [46]. He first introduced an integrate-and-fire neurone model without leak and showed that this neurone could respond equally well at any frequency, due to the fact that the firing probability is exactly proportional to the instantaneous synaptic current flowing to the neurone, as long as that current is positive. Thus, $\nu_1(\omega) = \text{constant}$, and the population is able to reproduce perfectly the time course of input stimuli.

He further showed that integrate-and-fire neurones with leak would show divergences at frequencies multiple of background firing rate (a resonance phenomenon). This introduces distortions in the response of the system to a stimulus. Neurones tend to prefer their intrinsic frequency and amplify the components of the signal at that frequency at the expense of others.

Knight then studied the response of the population with an extremely simplified noise model (drawing at random the threshold after each spike) and showed how it could decrease the size of the resonant peaks in the response of the neurone.

3.2.2. White noise

The response of a population of cells receiving a white noisy input plus a sinusoid with small amplitude has been computed in [14, 15]. The main features of the firing probability response are

- The amplitude peaks at frequencies multiple of the background firing rate ν_0 for small amplitude of the noise σ, much as in [46]. These peaks are less pronounced as the background frequency decreases;
- The amplitude decays as $1/\sqrt{\omega}$ for large ω;
- There is a phase lag of the response in firing probability that goes to a limit of 45 degrees for large ω.

These features are shown in the graphs of *figure 8*. Interestingly, these curves reproduce quite well curves measured using the same protocol in real neurones [22]. The two last features are peculiar to the white noise, as will be shown in the next section.

3.2.3. Synaptic (coloured) noise

Coloured noise dramatically changes the high frequency behaviour [14]. Intuitively, synaptic noise with time constant τ' interpolates between two limits: in the limit $\tau' = 0$, noise is white, and from the results exposed in the last section we expect that the amplitude of the response tends to zero at high frequency as $1/\sqrt{\omega}$. In the opposite limit, $\tau' \to \infty$, the fluctuations of the synaptic input around its mean vanishes, and in that limit the synaptic input becomes deterministic. In that limit, the amplitude of the firing probability response stays finite at arbitrarily high frequencies [46]. Thus, we expect the time constant of the synaptic noise to have a strong effect on the high frequency response.

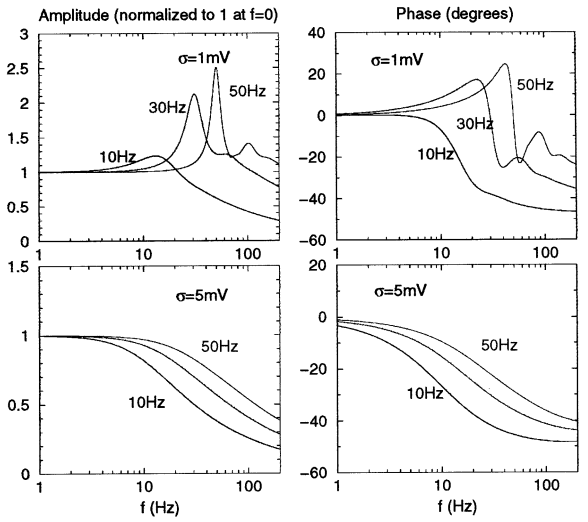

Figure 8. Amplitude and phase lag of the DC modulation in the population firing rate vs. frequency of the DC modulation in the input. Curves are normalized to 1 at zero frequency. The top graphs correspond to low noise amplitude ($\sigma = 1$ mV) while the bottom graphs correspond to high noise amplitude ($\sigma = 5$ mV).

Recently, the effect of a small synaptic time ($\tau' \ll \tau$) on the frequency response of an integrate-and-fire neurone has been studied analytically [14]. The integrate-and-fire neurone now obeys to the following equations,

$$\tau \frac{dV}{dt} = -V + \mu + \mu_1 \cos(\omega t) + I_{\text{noise}}$$

$$\tau' \frac{dI_{\text{noise}}}{dt} = \eta(\tau) - I_{\text{noise}}$$

where η is a white noise with zero mean and variance density σ^2. The analysis uses the two-dimensional Fokker-Planck formalism of Section 3.1.2. A solution is computed by expanding the equation around the white noise limit. The first order in $\sqrt{\tau'/\tau}$ yields

$$|\nu_1(\omega)| \to \nu_0 \sqrt{\frac{\tau'}{\tau}} \text{ when } \omega \to \infty$$

The high frequency limit of the phase lag is zero for any finite τ', indicating a discontinuity at $\tau = 0$. Furthermore, numerical simulations indicate that for sufficiently large σ and sufficiently large τ'/τ, the response $\nu_1(\omega)$ becomes independent of the frequency ω, with a phase lag close to zero. Thus, in that situation, population firing rate would reproduce perfectly and instantaneously variations in injected currents [14].

3.3. Sparsely connected network of two populations

When feedback is present the statistics of the synaptic inputs to the population become influenced by the activity of the population itself. Thus, the moments of the synaptic inputs and firing rates have to be related in a self-consistent way.

3.3.1. Stationary states

A population of cells receiving a synaptic input with mean μ_0 and variance σ_0^2 has a mean firing rate

$$\frac{1}{\nu_0} = \tau_{rp} + \tau\sqrt{\pi} \int_{\frac{V_r - \mu_0}{\sigma_0}}^{\frac{\theta - \mu_0}{\sigma_0}} du \exp(u^2)(1 + \text{erf}(u)) \qquad (4)$$

In a recurrent network, both μ_0 and σ_0^2 have two components, external and recurrent:

$$\mu_0 = \tau J(C_{\text{ext}}\nu_{\text{ext}} + C_E\nu_E - gC_I\nu_I) \qquad (5)$$

$$\sigma_0^2 = \tau J^2(C_{\text{ext}}\nu_{\text{ext}} + C_E\nu_E + g^2C_I\nu_I) \qquad (6)$$

Inserting Eq. (4) and Eq. (5) in Eq. (6), gives a self-consistent equation for the firing rates of the network [5].

This equation can be solved numerically to obtain the characteristics of stationary states of the network, as a function of the balance between the different components of the network: inhibitory vs. excitatory; and external vs. firing threshold for single cells. Results are shown for a large network ($C_E = 4\ 000$, $C_I = 1\ 000$) in *figure 9*.

There are five regions in this graph, depending on the inhibitory/excitatory balance, and the magnitude of the external inputs. In the excitatory dominated region, the system always has a high activity (close to saturation) fixed point, because of the strong excitatory feedback. When external inputs are sub-threshold, there is bistability between the quiescent state and the high activity state. The activity drops sharply at the balance point ($g \sim 4$). In the inhibitory-dominated regime, there are three regions: when external inputs are supra-threshold, the system is in a low activity state. Sufficiently sub-threshold, the quiescent state is stable. Close to threshold, there is a bistable region with coexistence between a low activity and a quiescent fixed points. The CV shows that firing is necessarily very regular in the excitatory dominated regime, while it is extremely irregular in the inhibition-dominated regime, with a sharp transition at $g \sim 4$.

3.3.2. Linear stability analysis: transitions towards synchrony, oscillations

Stability of the stationary states can be checked using linear stability analysis [12, 15]. This is done by determining solutions of the equations which are small perturbations of the form $\exp(\lambda t)$, where λ is complex, around the stationary state: $\nu = \nu_0 + \nu_1 \exp(\lambda t)$, $\mu = \mu_0 + \mu_1 \exp(\lambda t)$, $\sigma^2 = \sigma_0^2 + \sigma_1^2 \exp(\lambda t)$. A solution to the linearized equations with a positive real part, implies that an instability develops from that state. Network parameters for which $\mathrm{Re}(\lambda) = 0$ thus signal a bifurcation.

The perturbation in the population rate ν_1 is given by

$$\nu_1 = \nu_1^{\mu}(\lambda)\frac{\nu_0}{\sigma_0}\mu_1 + \nu_1^{\sigma}(\lambda)\frac{\nu_0}{\sigma_0^2}\sigma_1^2$$

in which $\nu_1^{\mu}(\lambda)$ is the linear response in changes to mean synaptic inputs, and $\nu_1^{\sigma}(\lambda)$ is the linear response in changes to the noise.

In a recurrent network, μ_1 and σ_1 depend in turn linearly on ν_1:

$$\mu_1 = \tau J(C_E - gC_I)\nu_1 \exp(-\lambda\delta)$$
$$\sigma_1^2 = \tau J(C_E - g^2 C_I)\nu_1 \exp(-\lambda\delta)$$

and thus

$$1 = \nu_1^{\mu}\frac{\mu_{0,\mathrm{rec}}}{\sigma_0}\exp(-\lambda\delta) + \nu_1^{\sigma}\frac{\sigma_{0,\mathrm{rec}}^2}{\sigma_0^2}\exp(-\lambda\delta) \qquad (7)$$

where $\mu_{0,\mathrm{rec}}$ and $\sigma_{0,\mathrm{rec}}$ are the components in the moments of the synaptic inputs coming from the recurrent collaterals. If a solution λ to Eq. (7) with $\mathrm{Re}(\lambda) > 0$, the stationary state is unstable. An oscillatory instability with frequency $\mathrm{Im}(\lambda)$ develops [12, 15].

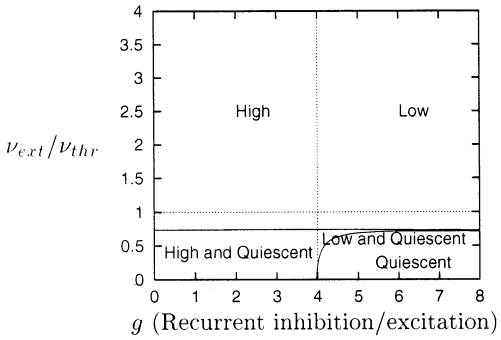

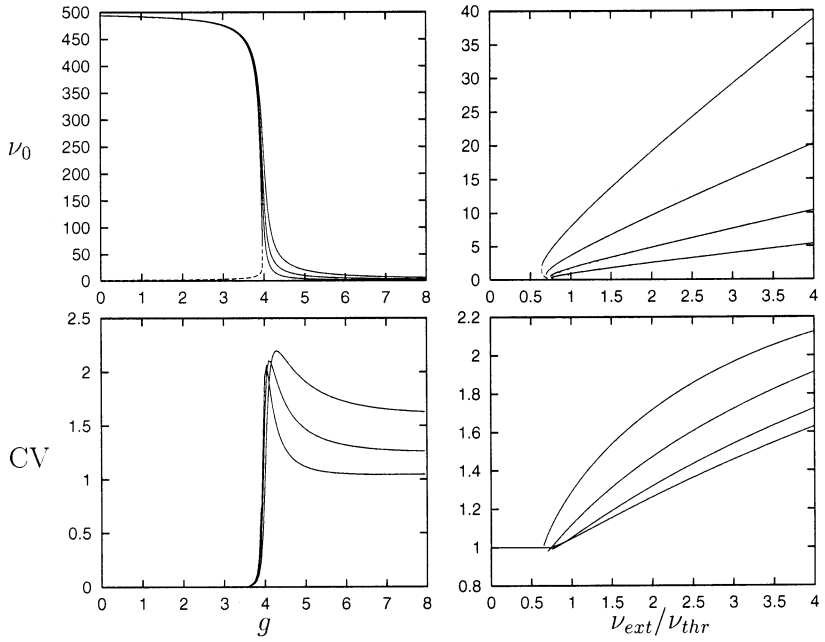

Figure 9. Characteristics of the stationary (asynchronous) state. Parameters: $C_E = 4\ 000$, $J = 0.2$ mV. Left: Bifurcation diagram of the system, in which saddle node bifurcations only are drawn (full lines). The vertical dotted line at $g = 4$ corresponds to the 'balanced' network in which feedback excitation and inhibition exactly cancel. Top graphs, left: firing rate in the High ($g < 4$) and Low ($g > 4$) activity states as a function of g, for $\nu_{ext}/\nu_{thr} = 0$, 1, 2, 4 (from bottom to top). Right: firing rate in the Low ($g > 4$) activity state as a function of ν_{ext}/ν_{thr}, for $g = 4.5$, 5, 6 and 8 (from top to bottom). Note the almost linear trend. Bottom graphs, left: Coefficient of variation (CV) of the ISI as a function of g. Note the sharp rise from $\mathrm{CV} \sim 0$ for $g < 4$ to values greater than one for $g > 4$. Right: Coefficient of variation (CV) of the ISI as a function of ν_{ext}/ν_{thr}.

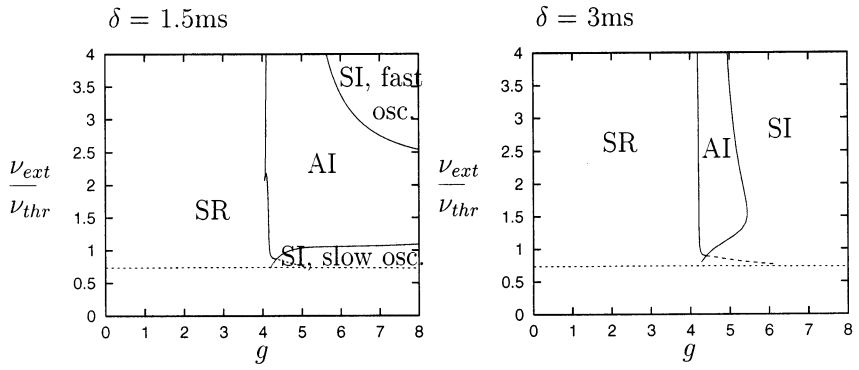

Figure 10. 'Phase diagrams' of the system, for two values of the synaptic delay, indicated on the corresponding picture. In each case the asynchronous, stationary state is stable in the region marked AI (irregular firing, $g > 4$), bounded by the Hopf bifurcation curves, indicated by full lines. On the Hopf bifurcation curves an oscillatory instability appears, and one enters either a SR state (synchronous regular firing) when excitation dominates, or SI states (synchronous irregular firing) when inhibition dominates. The short-dashed lines indicate the on which the almost quiescent stationary state destabilizes. It is stable below the line. In the small triangular region between SR and SI states, the network settles in a quasi-periodic state in which the global activity exhibits a fast oscillation on top of a slow oscillation, and individual neurones fire irregularly.

The boundaries of the region of stability of the asynchronous stationary state can be determined by solving numerically Eq. (7). The boundaries separate asynchronous from synchronous states. They are shown in *figure 10* for two values of the synaptic delay. Note that three types of instabilities appear. Close to the 'balance' line $g = 4$, an instability with a very high frequency appears, and the network settles in a highly synchronized state in which neurones fire at high frequencies. In the inhibitory-dominated region, two types of instabilities are present for small synaptic delays. These two regions merge when the synaptic delay is large enough. When external inputs are much larger than threshold, an oscillatory instability whose frequency is governed by the synaptic delay (a 'fast' oscillation) appear. Note that the firing rate of the neurones is independent and typically much smaller than the network frequency, in contrast to oscillatory states in regularly firing neurones. When external inputs are close to threshold, an oscillatory instability appears with a smaller frequency (a 'slow' oscillation), controlled by the membrane time constant.

In summary, the collective states of the network can be classified in four different types, depending on both global and individual behaviour. The global behaviour can be either asynchronous or synchronous, depending on whether solutions of Eq. (7) with positive real part can be found or not. Individual behaviour can be regular or irregular, depending on whether the CV is close to zero or close or higher than one. Thus, four types of collective behaviours can be identified: Asynchronous Irregular (AI); Asynchronous Regular (AR); Synchronous Irregular (SI); Synchronous Regular (SR).

Figure 11 illustrates with numerical simulations the nature of the different collective states identified by the analysis.

3.3.3. Beyond linear stability

To better understand the nature of the synchronous states close to the bifurcation line, a weakly non linear analysis can be performed [15]. This weakly nonlinear analysis consists in obtaining the terms up to third order in the perturbation analysis. Third order is necessary to determine the lowest order terms that saturate the instability that appears at first order.

The main result of the analysis consists in determining the deviation n_1 of the instantaneous spike rate from the stationary rate

$$n_1(t) = \hat{n}_1(t)\exp(i\omega_c t) + \hat{n}_1^*(t)\exp(-i\omega_c t)$$

close to the bifurcation $\hat{n}_1$ is a complex number that determines both the amplitude of the collective oscillation, and how its frequency varies when the system goes away from the instability line. $\hat{n}_1$ is given by a reduced equation of the form

$$\frac{d\hat{n}_1}{dt} = A\hat{n}_1 - B|\hat{n}_1|^2\hat{n}_1$$

where A and B are complex parameters that depend on network parameters. A vanishes on the bifurcation lines. In the inhibition dominated

regime, at the bifurcation point $\mathrm{Re}(B) > 0$. This means that the system undergoes a supercritical, or continuous, Hopf bifurcation when $A = 0$. Thus, very close to the line, an oscillatory instability with small amplitude develops. Going further away from the line in the synchronous region (for example increasing the external inputs), the amplitude of the global oscillation increases as the square root of the difference between the control parameter and its critical value. As an example, consider the diagram of *figure 11*. For $g = 6$, the system is in the asynchronous irregular state when the external frequencies range from about ν_{thr} to $3\nu_{\mathrm{thr}}$. If the external frequency is increased above the critical frequency of about $3\nu_{\mathrm{thr}}$, a global oscillation develop, with an amplitude which will be proportional to the square root of the difference between the external frequency and $3\nu_{\mathrm{thr}}$.

3.3.4. *Finite size effects*

In the simulations of *figure 11*, one sees that the global activity is not quite as predicted by the analysis. In the asynchronous, stationary state, large and irregular variations of the global activity can be seen, while in the oscillatory states, the oscillation is also quite irregular, with a phase diffusion phenomenon clearly visible. These features are due to finite size effects, or more precisely to the finite connection probability. The effect of a finite connection probability on network dynamics can also be estimated analytically [15]. It can be shown to introduce a stochastic term in the reduced equation

$$\frac{\mathrm{d}\hat{n}_1}{\mathrm{d}t} = A\hat{n}_1 - B|\hat{n}_1|^2\hat{n}_1 + D\zeta(t)$$

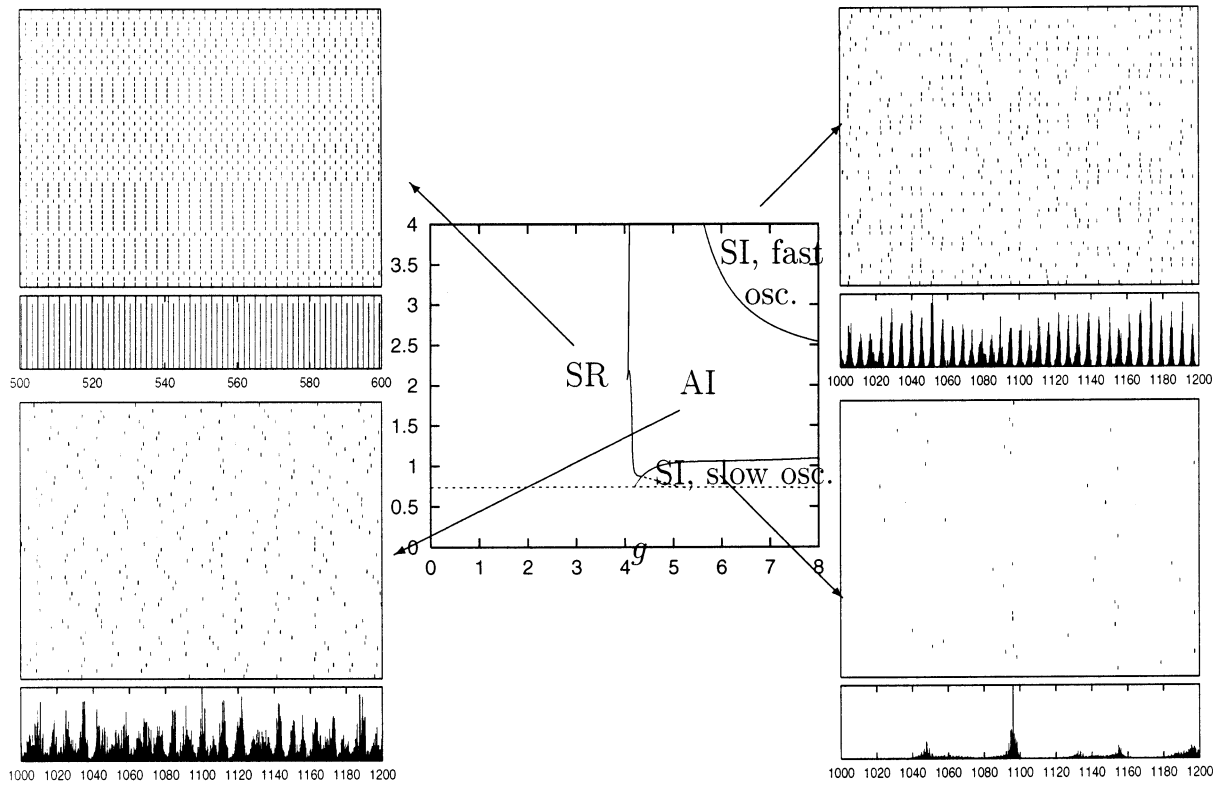

Figure 11. Simulations of a network of 10 000 pyramidal cells and 2 500 interneurones illustrate the different types of collective states, or 'phases' of the system. For each of the four examples are indicated the temporal evolution of the global activity of the system (instantaneous firing frequency computed in bins of 0.1 ms), together with the firing times (rasters) of fifty randomly chosen neurones. In the SR state, the network is almost fully synchronized and neurones fire regularly at high rates. In the fast oscillatory SI state, there is a fast oscillation of the global activity, and neurones fire irregularly at a rate which is lower than the global frequency. In the AI state, the global activity is stationary (fluctuations seen in the graph are a finite size effect, see Section 3.3.4), neurones fire irregularly. In the slow oscillatory SI state, there is a slow oscillation of the global activity, and neurones firing irregularly at very low rates.

This noise amplitude D is proportional to the square root of the connection probability ε. This noise term gives rise to the irregularity seen in the temporal evolution of the global activity.

3.4. Working memory in recurrent networks

This section deals with the dynamics of networks with structure in the synaptic matrix as introduced in Section 2.6.1. In the present section, it is assumed that the network is initially in an asynchronous irregular state, since this is the state that bears most resemblance with neocortical networks in the awake monkey during spontaneous activity (low firing rates, irregular spike trains, no prominent global oscillation).

To probe the effect of synaptic structure on the collective states of the network, the parameter w_+, measuring the relative strength of synapses connecting two excitatory neurones responding to the same object, is varied. The parameter w_- is varied so that spontaneous activity of the network does not change as w_+ is varied. *Figure 12* shows the firing rates of the spontaneous and persistent activities as a function of w_+. The middle branch connecting the two represents an unstable state. When w_+ is smaller than about 2.04, recurrent synapses are not strong enough to generate and sustain elevated persistent activity. Spontaneous activity is the only stable state. When w_+ becomes larger than about 2.04, persistent activity states appear. The network becomes 'multistable'. When w_+ is larger than about 2.3, recurrent excitation becomes too strong and the low spontaneous state becomes unstable and disappears. Below $w_+ \sim 2.3$, spontaneous activity remains constant as w_+ is varied. This is due to the fact that the 'average' excitatory synaptic efficacy remains constant, as w_- has been chosen to balance the potentiated synapses. Moreover, persistent activity increases with w_+, because the excitatory feedback within a selective population is directly proportional to w_+. The spontaneous and persistent states are separated by the unstable state (middle branch, dashed line in *figure 12*). The network is expected to converge to the spontaneous state (resp. persistent state) if it is initially below (resp. above) the unstable state. As w_+ increases, the difference in firing rate between the unstable state and persistent state (resp. spontaneous state) increases (resp. decreases). The persistent state becomes more stable at the expense of the spontaneous state, until spontaneous activity destabilizes when $w_+ \sim 2.30$.

In a finite network, both spontaneous and persistent activity states are not truly stable, in the sense that external noise might provoke after a very long time transitions towards different states, e.g. if one waits for long enough, random fluctuations might provoke spontaneous transitions from the spontaneous activity state to one of the memory states, and vice versa. When w_+ is not very close to the boundaries of the multistability range, the 'lifetimes' of both states are typically very long, i.e. larger than several seconds.

3.5. Spatial working memory

The present section describes a scenario similar to the last section, but in the spatial working memory architecture described in Section 2.6.2.

3.5.1. Structure of phase space in the spatial case

In the spatial case, the 'phase space' of the network is no longer composed of discrete attractors as in the object case (*figure 13*). Rather, when the parameter measuring synaptic structure w_+ is larger than some critical level, a continuous attractor forms which has the topology of a circle. The meaning of a point on that circle is that network activity profile is peaked on neurones which are selective to that particular orientation. All the points on the circle are attractors of the system, but they are only marginally stable with respect to translations on the circle.

3.5.2. Simulation of the delayed spatial task

The delayed oculomotor task [30] has been simulated in a network with 'realistic' synaptic characteristics (see Methods in [24]). A typical simulation is shown in *figure 14*. It consists of a cue presentation (C) followed by a delay period (D) and a response period (R). In brief, after the inter-trial interval, a cue is presented to a monkey at one of eight different locations separated by 45°. A delay period follows in which the monkey needs to maintain the cue location in working memory. Finally, upon extinction of a fixation target, the monkey is required to make a saccade to where the cue had been presented. A successful saccade brings a reward. This protocol was implemented in the following way: during cue presentation (C), a subpopulation of cells whose preferred cue was close to the stimulus location received transient external inputs. This

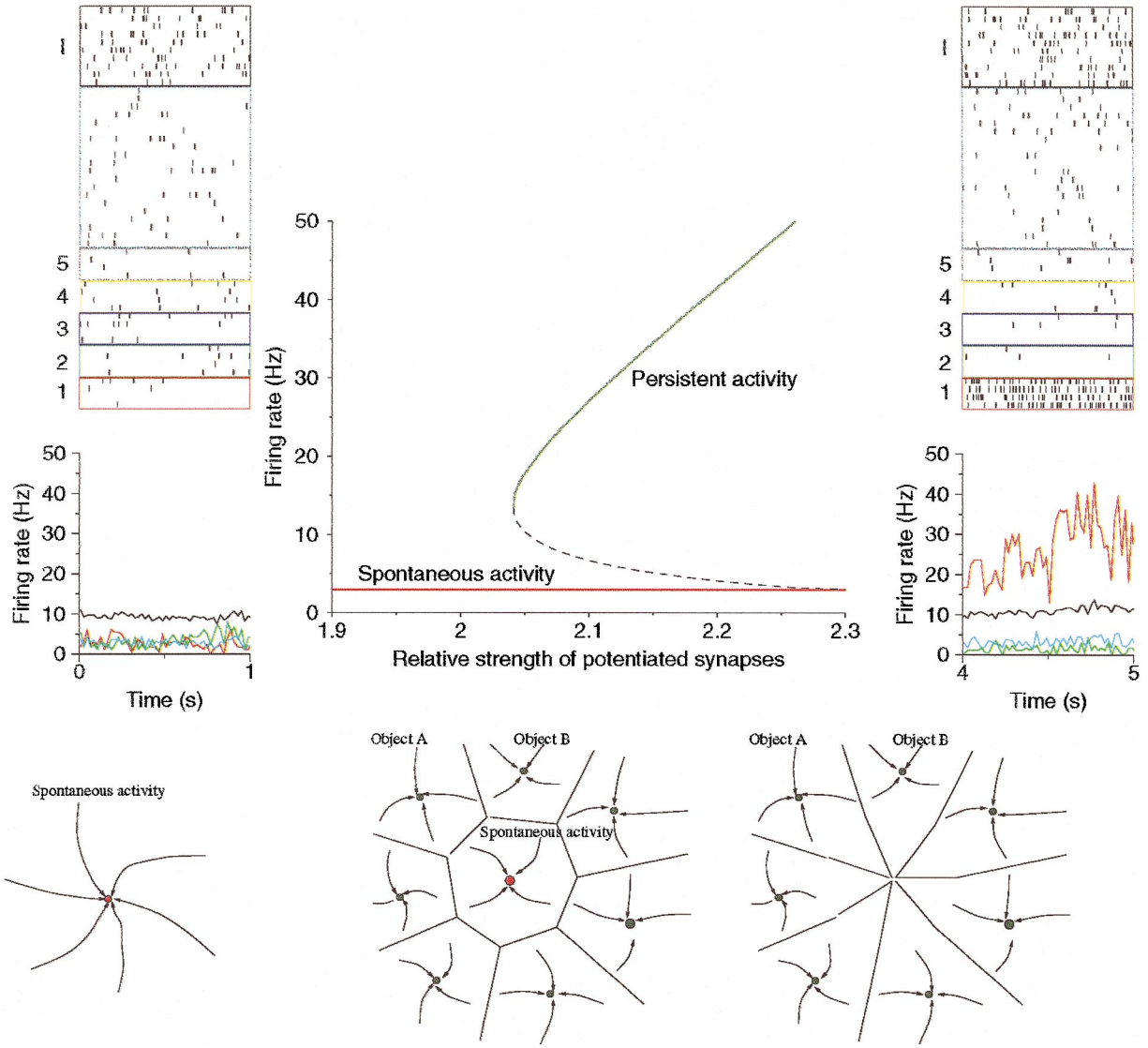

Figure 12. Top: at the centre, a graph shows how activity in a subpopulation coding for an object depends on the strength of potentiated synaptic connections w_+. It shows two stable branches, one corresponding to spontaneous activity, the other to persistent memory activity. An unstable branch, shown with a dashed line, indicates the boundary of the basins of attraction of spontaneous and persistent activity. To the left of the graph, a simulation of the spontaneous activity state in a network with 1 000 cells and $w_+ = 2.1$. To the right of the graph, a simulation of the persistent activity state in the same network. The network can switch from one state to another using transient selective external inputs to the subpopulations coding for a particular object. Bottom: schematic representation of the 'phase space' of the network. Left, below $w_+ \sim 2.05$, the network has a single fixed point attractor, the spontaneous activity state. Above this critical value, many additional attractors form, corresponding to the objects 'stored' in the synaptic matrix (centre). Last, a second bifurcation occurs at $w_+ \sim 2.3$ at which the spontaneous activity state becomes unstable (right).

selective input was removed during the delay period (D). Finally, during the response period (R), a non-specific transient input was applied to all cells of the network, simulating the effect of the motor response and reward.

In *figure 14*, spatiotemporal activity is smoothed and shown in a continuous and colour-coded map. The main features of network activity can be read out from this graphs from left to right. First, before cue presentation, neurones show sponta-

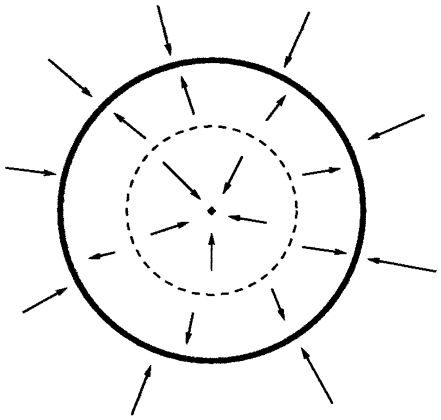

Figure 13. Schematic graph of the 'phase space' in the spatial working memory model.

neous activity at a few spikes per second. This activity is uniform in space: The network is untuned. Second, during the cue period (C), a pattern of increased activity develops around the location of the cue (180°). This increased activity is due to the external input to the subpopulation of neurones with preferred cues closest to the cue stimulus Third, in the delay period (D), the network initially localized response widens and stabilizes. The elevated persistent activity remains restricted to a selective neural subpopulation throughout the delay period. This is quantified by the peaked network profile of the averaged delay-period activity. The enhanced persistent rates (about 20 Hz) persist due to the strong excitatory feedback between cells sharing similar tuning properties. The tuned persistent activity profile is independent of the precise shape (or intensity) of the cue stimulus. Such a 'bump state' is an 'attractor' of network dynamics.

Finally, during the response period (R), a transient and overall increase of external inputs to the whole network leads to a transient increase of neuronal firing, which turns off the persistent activity [31, 35]. This 'switching-off' of persistent activity by excitation is due to the strong inhibitory feedback. A global excitatory drive to the network increases the firing rate of inhibitory cells in a way that is strong enough to effectively wipe out persistent activity and refresh the short-term memory.

3.5.3. Random drift

As can be expected in a noisy system, the memory of a spatial location drifts slightly and slowly away from the shown location, as can be shown in *figure 14*. Indeed, since the system is noisy, and the location of the bump is only marginally stable with respect to translations along the circle, noise produces a small random drift of the bump location. This will result in an error in the location of the bump that will increase linearly with time, as shown in *figure 15*.

4. Discussion and conclusions

The present paper has reviewed systematic investigations of various aspects of recurrent network dynamics that might shed light on some issues in theoretical or experimental neuroscience.

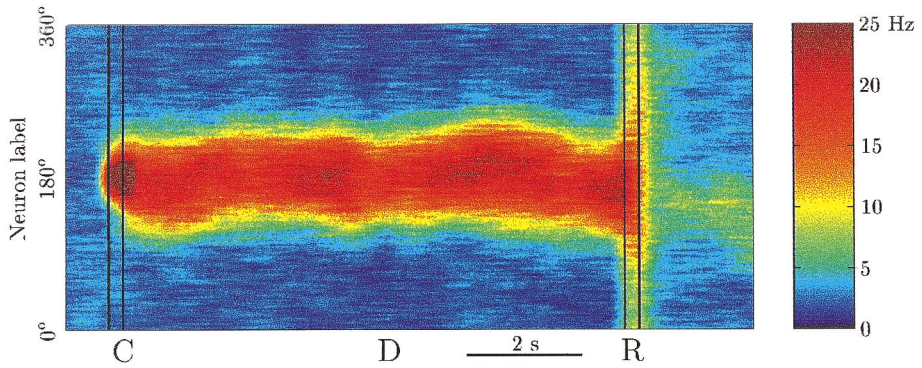

Figure 14. Working memory maintained by a tuned network activity state (a 'bump state'). C: cue period (250 ms, peak stimulus 200 pA), D: delay period (8.75 s), R: response period (250 ms, external current increase 500 pA). Colour coded spatiotemporal activity pattern. Note the enhanced and localized neural activity that is triggered by the cue stimulus and persists during the delay period. In these simulations, inhibitory interneurones (not shown) display a spontaneous activity rate of 9 Hz and an increased delay activity rate of 13 Hz. Adapted from [24].

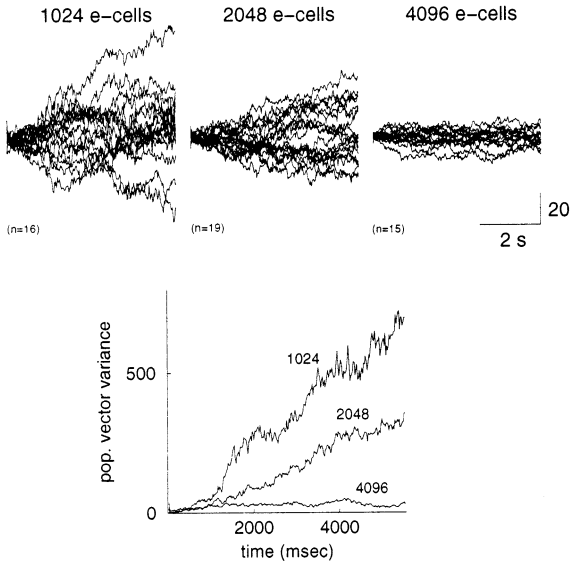

Figure 15. The network pattern of persistent activity drifts randomly in time due to noise. Upper panels: Population vector position versus time for different runs and different network sizes. Lower panels: Variance of the population vector position around the initial stimulation point averaged across trials and plotted versus time for each of the three network sizes studied. Note the linear trend, similar to a diffusion process. Adapted from [24].

In particular, a long standing issue in theoretical neuroscience is whether it is possible to describe the dynamics of a population of spiking neurones by simple firing rate formulations. In traditional 'firing rate' formulations (e.g. [42, 75]), the dynamics of the activity of a population of cells is described by equations of the type

$$\tau \dot{\nu} = -\nu + \phi(\mu,\sigma)$$

Consequently, 'firing rate neurones' have low-pass filter properties. Responses to stimuli with high frequency decay as $\sim 1/(\omega\tau)$.

By contrast, results of Section 3.2 show that networks of noisy 'spiking' neurones show much less ($\sim 1/\sqrt{\omega\tau}$) or no attenuation at all at high frequencies. Thus, this allows for a much faster dynamics than networks of 'firing rate' neurones.

Unfortunately, it is not possible in general to perform a simple reduction from 'spiking' to 'firing rate' dynamics, except in two limit cases:

1. When background rates are extremely low background rates, and noise is white, the linear response tends to the one of a low pass filter governed by the membrane time constant. Thus, in that limit, the system could be described by firing-rates equations a la Wilson-Cowan.
2. When background rates are high enough, and a strong coloured noise is present, as might be the case in neocortical networks, the response to variations in the inputs can in principle be instantaneous. The response to inputs coming through synapses will be governed by synaptic time constants. For inputs coming through fast AMPA synapses, this means that the characteristic time of the response will be much faster than the one of a 'firing-rate' neurone (see also [65]).

Studies of the response dynamics of neural populations points to interesting functional consequences of background activity and noise in neural populations: if background activity is high enough, and noise has a long enough correlation time, the system will be able to react instantaneously to changes in input stimuli.

The present paper also emphasizes that recurrent connections typically generate interesting dynamical features. As hypothesized by several authors [5, 67], an excitation-inhibition balance due to strong recurrent inhibition is useful to settle the network in a low rate, irregular state. van Vreeswijk and Sompolinsky [70] showed that such a state was indeed stable in a network of binary neurones. Later, Brunel and Hakim [12, 15] showed that in a sparsely connected network of integrate-and-fire neurones, this asynchronous irregular state (or chaotic balanced state) was indeed stable in a large parameter range, when recurrent inhibition is strong enough.

The Asynchronous Irregular state shows many similarities to 'spontaneous activity' in vivo, because of irregular firing at low rates, and no obvious temporal structure in population activity. The Synchronous Irregular state bears also similarity to oscillatory states seen in vivo. Indeed, there is evidence for irregular activity at low rates during global oscillations in the hippocampus of the rat during the 200-Hz oscillations in vivo [19, 25], and in both hippocampal and neocortical slices during carbachol and/or kainate induced 40-Hz oscillations [18, 29]. The frequency of the oscillation depends strongly on the IPSC decay time in the 40-Hz oscillation in vitro [29], as in the sparsely connected network in the fast oscillatory regime described here. Global oscillation frequency, average firing rates of E and I cells and phase lag between excitatory and inhibitory populations as observed in the hippocampus can be obtained using appropriate synaptic parameters [17].

Transitions between AI and SI states are typically observed in the model by an increase in external inputs. Again, this bears similarity with the experimental data both in vivo or in vitro. Indeed, oscillations are often provoked by an increase in external inputs or an increase in excitability. The 40-Hz rhythm in vitro is induced either by carbachol [29], that increases the excitability of both pyramidal cells and interneurones, or by a combination of carbachol and kainate [18]. 200-Hz oscillations in CA1 in vivo are thought to be due to a massive depolarization through Scaheffer collaterals [19]. Such a massive increase in external inputs is consistent with a transient increase in firing rates during sharp waves [25].

In the model, oscillations disappear when the inhibitory feedback decreases. This feature seems again similar to the pharmacology of 40-Hz rhythms in vitro, that are readily abolished by a blockade of GABA receptors by bicuculline [18, 29].

Last, working memory networks described in the present paper have many interesting properties and striking similarities with the available experimental data on delayed response tasks in monkeys. Here, due to lack of space, I have chosen to focus on the random drift property in spatial working memory networks. For other aspects, see [3, 24, 76]. The random drift observed in the model predicts an error in the memorized position whose variance grows quadratically with time. Errors have been measured in tasks when a saccade has to be made to a memorized position in both monkeys [73] and humans [54]. For small delay periods, the variance of the error does increase linearly with time, as predicted by the simple spatial working memory model presented here. For longer delay periods, a sub-linear trend can be seen, indicating that the observed drift is smaller that what would be predicted by a purely diffusive model.

Acknowledgements

I would like to thank Larry Abbott, Daniel Amit, Frances Chance, Albert Compte, Paolo del Giudice, Boris Gutkin, Stefano Fusi, Vincent Hakim, Massimo Mascaro, Maurizio Mattia, Jesper Tegner and Xiao-Jing Wang for useful discussions related to dynamics of neurones and networks.

References

[1] Abbott L.F., van Vreeswijk C., Asynchronous states in a network of pulse-coupled oscillators, Phys. Rev. E 48 (1993) 1483–1490.

[2] Amit D., Modeling Brain Function, Cambridge University Press, 1989.

[3] Amit D., Brunel N., Tsodyks M.V., Correlations of cortical hebbian reverberations: experiment vs theory, J. Neurosci. 14 (1994) 6435–6445.

[4] Amit D.J., Brunel N., Learning internal representations in an attractor neural network with analogue neurons, Network 6 (1995) 359–388.

[5] Amit D.J., Brunel N., Model of global spontaneous activity and local structured activity during delay periods in the cerebral cortex, Cerebral Cortex 7 (1997) 237–252.

[6] Amit D.J., Fusi S., Dynamic learning in neural networks with material sysnapses, Neural Comput. 6 (1994) 957–982.

[7] Amit D.J., Gutfreund H., Sompolinsky H., Storing infinite numbers of patterns in a spin-glass model of neural networks, Phys. Rev. Lett. 55 (1985) 1530–1531.

[8] Amit D.J., Tsodyks M.V., Quantitative study of attractor neural network retrieving at low spike rates I: substrate-spikes, rates and neuronal gain, Network 2 (1991) 259–274.

[9] Ben-Yishai R., Lev Bar-Or R., Sompolinsky H., Theory of orientation tuning in visual cortex, Proc. Natl. Acad. Sci. USA 92 (1995) 3844–3848.

[10] Bernander O., Koch C., Usher M., Synaptic background activity determines spatio-temporal integration in single pyramidal cells, Proc. Natl Acad Sci USA 88 (1991) 11569–11573.

[11] Bethge M., Pawelzik K., Rothenstein R., Tsodyks M., Noise as signal for neuronal populations, Phys. Rev. Lett. (2000) (submitted).

[12] Brunel N., Dynamics of sparsely connected networks of excitatory and inhibitory spiking neurons, J. Comput. Neurosci. 8 (2000) 183–208.

[13] Brunel N., Carusi F., Fusi S., Slow stochastic Hebbian learning of classes in recurrent neural networks, Network 9 (1998) 123–152.

[14] Brunel N., Chance F., Fourcaud N., Abbott L., Effects of synaptic noise and filtering on the frequency response of spiking neurons, Phys. Rev. Lett. (2000) (submitted).

[15] Brunel N., Hakim V., Fast global oscillations in networks of integrate-and-fire neurons with low firing rates, Neural Comput. 11 (1999) 1621–1671.

[16] Brunel N., Sergi S., Firing frequency of integrate-and-fire neurons with finite synaptic time constants, J. Theor. Biol. 195 (1998) 87–95.

[17] Brunel N., Wang X.J., Fast network oscillations with intermittent cell firing in recurrent circuits, (2000) (in prep.).

[18] Buhl E.H., Tamas G., Fisahn A., Cholinergic activation and tonic excitation induce persistent gamma oscillations in mouse somatosensory cortex in vitro, J. Physiol. (Lond.) 513 (1998) 117–126.

[19] Buzsaki G., Urioste R., Hetke J., Wise K., High frequency network oscillation in the hippocampus, Science 256 (1992) 1025–1027.

[20] Camperi M., Wang X.-J., A model of visuospatial short-term memory in prefrontal cortex: recurrent network and cellular bistability, J. Comput. Neurosci. 5 (1998) 383–405.

[21] Chafee M.V., Goldman-Rakic P.S., Neuronal activity in macaque prefrontal area 8a and posterior parietal area 7ip related to memory guided saccades, J. Neurophysiol. 79 (1998) 2919–2940.

[22] Chance F., Ph.D. thesis, Brandeis University, 2000.

[23] Chow C., Phase-locking in weakly heterogeneous neuronal networks, Physica D 118 (1998) 343–370.

[24] Compte A., Brunel N., Goldman-Rakic P.S., Wang X.-J., Synaptic mechanisms and network dynamics underlying spatial working memory in a cortical network model, Cerebral Cortex 10 (2000) 910–923.

[25] Csicsvari J., Hirase H., Czurko A., Mamiya A., Buzsáki G., Oscillatory coupling of hippocampal pyramidal cells and interneurons in the behaving rat, J. Neurosci. 19 (1999) 274–287.

[26] Destexhe A., Mainen Z.F., Sejnowski T.J., Kinetic models of synaptic transmission, in: Koch C., Segev I. (Eds.), Methods in Neuronal Modeling, Second edn, MIT press, Cambridge, MA, 1998, pp. 1–25.

[27] Destexhe A., Paré D., Impact of network activity on the integrative properties of neocortical pyramidal neurons in vivo, J. Neurophysiol. 81 (1999) 1531–1547.

[28] Ernst U., Pawelzik K., Geisel T., Synchronization induced by temporal delays in pulse-coupled oscillators, Phys. Rev. Lett. 74 (1995) 1570–1573.

[29] Fisahn A., Pike F.G., Buhl E.H., Paulsen O., Cholinergic induction of network oscillations at 40hz in the hippocampus in vitro, Nature 394 (1998) 186–189.

[30] Funahashi S., Bruce C.J., Goldman-Rakic P.S., Mnemonic coding of visual space in the monkey's dorsolateral prefrontal cortex, J. Neurophysiol. 61 (1989) 331–349.

[31] Funahashi S., Bruce C.J., Goldman-Rakic P.S., Neuronal activity related to saccadic eye movements in the monkey's dorsolateral prefrontal cortex, J. Neurophysiol. 65 (1991) 1464–1483.

[32] Fuster J.M., Jervey J.P., Inferotemporal neurons distinguish and retain behaviourally relevant features of visual stimuli, Science 212 (1981) 952–955.

[33] Gerstner W., Time structure of the activity in neural network models, Phys. Rev. E 51 (1995) 738–758.

[34] Gerstner W., van Hemmen L., Cowan J., What matters in neuronal locking?, Neural Comput. 8 (1996) 1653–1676.

[35] Goldman-Rakic P.S., Funahashi S., Bruce C.J., Neocortical memory circuits, in: Cold Spring Harbor Symposia on Quantitative Biology, vol. LV, 1990, pp. 1025–1038.

[36] Golomb D., Hansel D., The number of synaptic inputs and the synchrony of large sparse neuronal networks, Neural Comput. 12 (2000).

[37] Hagan P.S., Doering C.R., Levermore C.D., Mean exit times for particles driven by weakly colored noise, SIAM J. Appl. Math. 49 (1989) 1480–1513.

[38] Hahnloser R.H.R., Sarpeshkar R., Mahowald M.A., Seung H.S., Digital selection and analogue amplification coexist in a cortex-inspired silicon circuit, Nature 405 (2000) 947–951.

[39] Hansel D., Mato G., Meunier C., Synchrony in excitatory neural networks, Neural Comput. 7 (1995) 307–337.

[40] Hebb D.O., Organization of Behavior, Wiley, New York, 1949.

[41] Hopfield J.J., Neural networks and physical systems with emergent collective computational abilities, Proc. Natl. Acad. Sci. USA 79 (1982) 2554–2558.

[42] Hopfield J.J., Neurons with graded response have collective computational properties like those of two-state neurons, Proc. Natl. Acad. Sci. USA 81 (1984) 3088–3092.

[43] Hopfield J.J., Herz A.V.M., Rapid local synchronization of action potentials: towards computation with coupled integrate-and-fire neurons, Proc. Natl. Acad. USA 92 (1995) 6655–6662.

[44] Jahr C.E., Stevens C.F., Voltage dependence of NMDA-activated macroscopic conductances predicted by single-channel kinetics, J. Neurosci. 10 (1990) 3178–3182.

[45] Klosek M.M., Hagan P.S., Colored noise and a characteristic level crossing problem, J. Math. Phys. 39 (1998) 931–953.

[46] Knight B.W., Dynamics of encoding in a population of neurons, J. Gen. Physiol. 59 (1972) 734–766.

[47] Miller E.K., Erickson C.A., Desimone R., Neural mechanisms of visual working memory in prefrontal cortex of the macaque, J. Neurosci. 16 (1996) 5154–5167.

[48] Mirollo R.E., Strogatz S.H., Synchronization of pulse-coupled biological oscillators, SIAM J. Appl. Math. 50 (1990) 1645–1662.

[49] Miyashita Y., Neuronal correlate of visual associative long-term memory in the primate temporal cortex, Nature 335 (1988) 817–820.

[50] Miyashita Y., Chang H.S., Neuronal correlate of pictorial short-term memory in the primate temporal cortex, Nature 331 (1988) 68–70.

[51] O'Scalaidhe S.P., Wilson F.A.W., Goldman-Rakic P.S., Areal segregation of face-processing neurons in prefrontal cortex, Science 278 (1997) 1135–1138.

[52] O'Scalaidhe S.P., Wilson F.A.W., Goldman-Rakic P.S., Face-selective neurons during passive viewing and working memory performance of rhesus monkeys: Evidence for intrinsic specialization of neuronal coding, Cerebral Cortex 9 (1999) 459–475.

[53] Pham J., Pakdaman K., Vibert J.F., Noise-induced coherent oscillations in randomly connected neural networks, Phys. Rev. E 58 (1998) 3610–3622.

[54] Ploner C.J., Gaymard B., Rivaud S., Agid Y., Pierrot-Deseilligny C., Temporal limits of spatial working memory in humans, Eur. J. Neurosci. 10 (1998) 794–797.

[55] Rapp M., Yarom Y., Segev I., The impact of parallel background activity on the cable properties of cerebellar purkinje cells, Neural Comput. 4 (1992) 518–532.

[56] Redish A.D., Elga A.N., Touretzky D.S., A coupled attractor model of the rodent head direction system, Network 7 (1996) 671–685.

[57] Ricciardi L.M., Diffusion Processes and Related Topics on Biology, Springer-Verlag, Berlin, 1977.

[58] Risken H., The Fokker Planck Equation: Methods of Solution and Applications, Springer-Verlag, Berlin, 1984.

[59] Sakai K., Miyashita Y., Neural organization for the long-term memory of paired associates, Nature 354 (1991) 152–155.

[60] Seung H.S., Lee D.D., Reis B.Y., Tank D.W., Stability of the memory of eye position in a recurrent network of conductance-based model neurons, Neuron 26 (2000) 259–271.

[61] Somers D.C., Nelson S.B., Sur M., An emergent model of orientation selectivity in cat visual cortical simple cells, J. Neurosci. 15 (1995) 5448–5465.

[62] Somogyi P., Tamás G., Lujan R., Buhl E.H., Salient features of synaptic organization in the cerebral cortex, Brain Res. Rev. 26 (1998) 113–135.

[63] Suzuki W.A., Miller E.K., Desimone R., Object and place memory in the macaque entorhinal cortex, J. Neurophysiol. 78 (1997) 1062–1081.

[64] Terman D., Wang D.L., Global competition and local cooperation in a network of neural oscillators, Physica D 81 (1995) 148–176.

[65] Treves A., Mean-field analysis of neuronal spike dynamics, Network 4 (1993) 259–284.

[66] Tsodyks M.V., Mit'kov I., Sompolinsky H., Pattern of synchrony in inhomogeneous networks of oscillators with pulse interactions, Phys. Rev. Lett. 71 (1993) 1280–1283.

[67] Tsodyks M.V., Sejnowski T., Rapid state switching in balanced cortical network models, Network 6 (1995) 111–124.

[68] Tuckwell H.C., Introduction to Theoretical Neurobiology, Cambridge University Press, Cambridge, 1988.

[69] van Vreeswijk C., Abbott L., Ermentrout G.B., When inhibition not excitation synchronizes neural firing, J. Comput. Neurosci. 1 (1994) 313–321.

[70] van Vreeswijk C., Sompolinsky H., Chaos in neuronal networks with balanced excitatory and inhibitory activity, Science 274 (1996) 1724–1726.

[71] van Vreeswijk C., Sompolinsky H., Chaotic balanced state in a model of cortical circuits, Neural Comput. 10 (1998) 1321–1371.

[72] Wang X.-J., Synaptic basis of cortical persistent activity: the importance of NMDA receptors to working memory, J. Neurosci. 19 (1999) 9587–9603.

[73] White J.M., Sparks D.L., Stanford T.R., Saccades to remembered target locations: and analysis of systematic and variable errors, Vision Res. 34 (1994) 79–92.

[74] Willshaw D., Buneman O.P., Longuet-Higgins H., Non-holographic associative memory, Nature 222 (1969) 960–962.

[75] Wilson H.R., Cowan J.D., Excitatory and inhibitory interactions in localized populations of model neurons, Biophys. J. 12 (1972) 1–24.

[76] Yakovlev V., Fusi S., Berman E., Zohary E., Inter-trial neuronal activity in inferior temporal cortex: a putative vehicle to generate long-term visual associations, Nature Neurosci. 1 (1998) 310–317.